Innovative unmanned aerial vehicle self-backhauling hybrid solution using RF/FSO system for 5G networks

Mohammad A. Massad, Baha' Adnan Alsaify, Abdallah Y. Alma'aitah

Department of Network Engineering and Security, Jordan University of Science and Technology, Irbid, Jordan

Article Info	ABSTRACT
	The impractical association of a dedicated fiber optic backhauling link with each base station in future wireless area network (WAN) networks promoted self-backhauling to become one of the most practical techniques for ultra-dense deployments. Self-backhauling reduces the number of stations with fiber-optic links, while the remaining stations can communicate with the core network through wireless multi-hoping connections. Nevertheless, routing through self-backhauling stations is an NP-hard problem. In this study, we propose a routing scheme based on a semi-distributed self-learning algorithm to reduce the end-to-end latency which achieve better stability against the dynamic nature of the mobile network, such as load variations and link failures. The proposed solution offers changing propagation medium between free-space optical (FSO) and radio frequency (RF); this dynamic change between every two hops reduces power consumption, increases throughput, and minimizes latency. Based on the performed simulation, our proposed algorithm measured better overall bit error rate (BER) compared to both RF-only and free-space optical FSO-only techniques resulting in increased backhauling capacity and reduced overall route interference.

Corresponding Author:

Baha' Adnan Alsaify
Department of Network Engineering and Security, Jordan University of Science and Technology
Irbid, Jordan
Email: baalsaify@just.edu.jo

1. INTRODUCTION

Today, many researchers show more interest in the cellular network, specifically those focusing on the millimeter-wave bands (mm-Wave) as a door to 5G networks. Such mm-Wave bands have a limitation in the communication distance for their short communication range due to high path loss and very high penetration loss through different obstacles such as the human body and buildings [1], [2]. To deal with such constraints, an ultra-dense deployment becomes essential for mm-Wave cellular networks to reduce the effect of these constraints [1], [2].

Furthermore, the backhaul in the mobile network connects the radio frequency (RF) tower at the cell sites to the corresponding core network, ensuring that the mobile users' connectivity is available. Normal backhauling in the current architecture is unscalable and it is not cost-effective to have a dedicated fiber-optic link connected to each base-station (BS) for mobile operators and having more locations to deploy these stationary base-stations. To find a solution for ultra-dense deployment, researchers are investigating the concept of self-backhauling [3]. In self-backhauling, the fiber-optic links connected to the core network are associated with a fewer number of selected base-stations (we refer to them as Fiber-BS in this work). The remaining base-stations are connected to the proposed Fiber-BS using wireless links operating using the industry-standard

wireless communication protocols.

The self-backhauling concept is defined in wireless communication by establishing backhaul links, which comprise all the intermediate network links (both wired and wireless connections links) between cell sites at the network edge with the corresponding core network. Besides, in self-backhauling, all the communication between the neighbor base-stations shares the same channels and spectrum as the communication between the mobile users and the corresponding stationary base-stations. Using self-backhauling leads to increased network capacity while keeping the installation and operational costs at the minimum.

The 5G mobile network is a new standard coming after the 4G network in the telecommunication industry to enable an unlimited number of devices and objects to be connected. It is using a wider spectrum such as sub-6 GHz and mm-Wave. The reason behind developing this technology is the need for a very high data communication speed, which could be up to multi-Gbps data rate, very low end-to-end latency with an ultra-high capacity to enable massive networks.

Every new technology comes with new challenges. For the 5G technology, the challenge arises from the underlying nature of the used technology mm-Wave, where it is suffering from high path loss of signal with high penetration loss, which results in making the signal affected by both dynamic and static types of blockage. To minimize these effects, it needs a densification deployment to ensure a sufficient level of an alternative route to access the core network through wireless communication between the available base stations. Figure 1 illustrates the self-backhauling comparing to fronthauling.
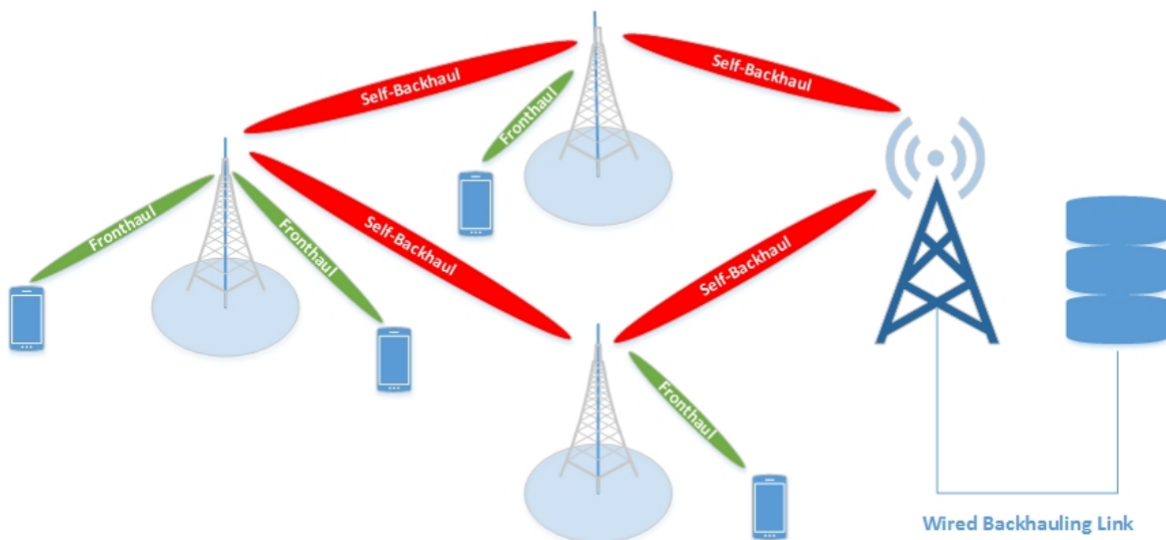

Figure 1. Self-backhauling and fronthauling

Challenges such as interference, computational complexity, quality-of-service (QoS), and robustness are present when the self-backhauled mm-Wave solution is deployed. Such challenges appear because of the high path lose of the mm-Wave and the need for ultra-dense deployment. It is essential for a self-backhauling system to use proper routing and scheduling algorithms. Using a routing algorithm that is designed for another environment may cause some problems. For example, using the shortest path algorithm may not be suitable for a self-backhauled system due to: i) huge number of users arrivals causing a packet drop and buffer overflow (e.g., a bus is crossing the cell), ii) temporary blockage because of moving objects (e.g., large vehicles or a mobile user crosses behind a large building), and iii) first and second-line interference from the surrounding base stations. One of the main components in the proposed system architecture is using unmanned aerial vehicle (UAV) as a self-backhualing base-station (S-BS). Furthermore, we introduce a new notion to enhance the overall system performance by mixing RF with free-space-optical (FSO) propagation media in an adynamic way while considering the different types of fading between every two consecutive hops in the selected route.

In this study, we addressed self-backhauling routing challenges in high altitude UAV networks with adaptive communication medium selection between FSO and RF. Due to the use of mm-Wave RF communi-

cation systems, many factors affect the choice of which medium to use in data transmission. For example, temporary obstacle blockage, pointing errors, and weather conditions are some of the factors that affect the decision of which medium to use. Even though the impact of these factors might be temporary [4], but their frequent occurrence might affect the cost of the selected route significantly in case the route is not adapted to mitigate these challenges.

The contribution of this work is to develop a routing scheme. We determine the route the data should take based on calculating the links' weight and selecting the appropriate path. The weight of the medium is based on the signal-to-noise ratio (SNR) value of each of the available paths. For RF medium, the SNR is modeled by Rayleigh and Gamma-Gamma distributions, while for FSO links, the SNR is measured taking into consideration the atmospheric disturbance and the pointing error fading across the available paths.

Our model is based on a scalable algorithm that uses a semi-distributed approach with artificial intelligence (AI) learning agents attached to every S-BS to provide scalability to the solution, taking into consideration the latency, interference, and traffic variation as well as the channel fluctuations. Within the proposed solution, we are using UAV as an S-BS rather than the commonly used RF base stations (BSs) while keeping the RF stationary BSs as a front hauling BSs. Furthermore, we are providing a hybrid selection mechanism to utilize the FSO over RF whenever it is possible.

Our proposed solution consists of two types of multi-level S-BS cellular network BSs: Fiber-BS as backhauled BSs (F-BSs) and self-backhauled BSs (S-BSs). Regarding F-BS, it is a stationary backhauling tower connected to the core network via a dedicated fiber-optic link, where the UAV S-BSs reach it via multi-hop wireless links, either using FSO or through RF communication based on the measured SNR value between every two hopes (UAV S-BS) on the selected route and the overall routes selection is based on the average bit error rate (BER). Each BS is equipped with a single RF and a single FSO interface. Within this paper, we are assuming that all RF communication is carried using the same RF bands. To evaluate the proposed solution, we rely on two metrics: first, we will evaluate the proposed algorithms by examining the computational complexity of each of them and calculate the overall performance using Big O notation ($O(f(n))$). Then, we will perform an extensive simulation to illustrate the reliability and robustness in different situations; and finally, we will compare the solution performance with a selected number of well-known techniques such as SCAROS, RT, and MTFS algorithms.

The rest of this paper is organized: section 2 shows the background and related work to this topic. Section 3 provides an overview of our proposed algorithm. Performance evaluation, analysis, obtained results, and a comprehensive discussion is presented in section 4. Finally, we give our conclusions in sections 5

2. RELATED WORK

As the world and telecommunication operators go beyond 4G and 5G networks, their objectives and goals are driven by their customers' needs. Mobile customers become in need of higher network capacity, bandwidth, throughput improvement, low latency, interference minimization, and decreasing in the measured BER to improve the QoS. Achieving these improvements requires new concepts and techniques to emerge with a great improvement in the network architecture itself. An example of these techniques is the ultra-dense deployment and mm-Wave utilization, which are considered as a prominent solution for these architectural improvements demands. To proceed in this paper, it is essential to give an overview of each of these used technologies and techniques.

2.1. Ultra-dense networks for 5G networks and beyond

To cope with the expected increase in the data traffic and due to the number of connected users as well the nature of the used applications, one of the main aspects that have to be taken into consideration is infrastructure densification. One of the main techniques to achieve infrastructure densification is ultra-dense network deployment [5]. The ultra-dense network deployment plays a significant role in this goal; it means that a large number of small cells have to be deployed to form a robust 5G network. But going with this technique potential will raise several new challenges related to mobility, backhauling, and interference. Table 1 shows an example of different dense deployment per cellular network.

To overcome these challenges, a new layer of network functionalities need to be implemented hierarchically. Besides that, the researchers in this field of study try to minimize the interference using different techniques such as inter-cell interference coordination or dynamic carrier selection in an autonomous way. All of the mentioned techniques are applicable in small cells environment, but still, it is prone to flexibility failure

[6] which makes them not suitable in the 5G and beyond networks; these networks need more flexibility, scalability, and lower interference [6]. For these types of challenges, a new emerging concept shows great potential in increasing the data rate while reducing the interference; this technique is called self-backhauling.

Table 1. Ultra dense in 5G cellular networks

Cellular network	Number of base stations
3G	$4 - 5/(km)^2$
4G	$8 - 10/(km)^2$
5G	$40 - 50/(km)^2$

2.2. Self-backhauling for 5G networks and beyond

Due to the increasing demand for data traffic, using mm-Wave becomes essential to enhance the data rate and throughput. However, when intended to use these frequency ranges, more system design challenges come to the surface, showing more need for network densification with efficient cost deployment. To figure out all these challenges, the concept of self-backhauling in cellular communication shows a promising result especially by increasing the network capacity while reducing the deployment cost [7]. The self-backhauling technique is defined in wireless communication between a BS and the next BS sharing the same resource that is already used between mobile users and their corresponding base station until reaching the core network. The main advantages of using this technique are increasing network capacity and reducing installation and operation costs.

2.2.1. Why self-backhauling?

When asking why we need the self-backhauling, the simple and straightforward answer is the high density of the deployed network to achieve better performance, increase the availability, and increase the scalability of the available backhaul links. Self-backhauling in a cellular network is the enabler of reducing the reliance on the wired backhaul for every deployed BS and the access node. As a result, it gives a simple and cost-effective deployment solution with better network planning and minimal deployment and operation efforts.

The advantages of using the self-backhauling can be summarized in the pointS;: i) better spectrum reuse efficiency between different BS and backhauling link, ii) cost efficiency resulting from sharing the same hardware. Which eventually result in reducing the running operation and maintenance cost, and iii) minimize the corresponding latency, which usually affects the transmission.

Utilizing the self-backhauling technique is a promising technique to solve most of the facing challenges. However, still, some challenges will be left unresolved especially that we are using mm-Wave. One of these challenges is the blockage percentage due to high penetration and path loss of the mm-Wave and the interference with the other self-backhauling BS. To overcome these challenges, the use of an UAV as a S-BS becomes important.

2.3. UAV as self-backhauling base station (S-BS)

Utilizing the UAVs in the telecommunication industry shows promising results in providing a solution for a large number of challenges, especially beyond 5G era. This utilization can help in increasing the backhauling network capacity with relatively low cost in both mobile and stationary users. In addition, UAV utilization will provide a high level of network flexibility in terms of coverage area and latency.

2.3.1. Why utilizing UAV as a S-BS?

When digging in this area, you can find many related works where they focus on using the UAV in three different ways [2], [8], and [9]. The first one is using the UAV as a normal base station and allowing mobile users to connect directly, and passing their traffic between these users and the core network directly Figure 2(a), and this is the most common focus. We believe that this technique can be useful in temporary events like frequent temporary blockage resulting from user or object mobility or by load amplification from a huge or sudden arrival of many users, which could interfere with the neighboring cell when trying to communicate ground and aerial BS. The second focused area is using the UAV as front hauling where it acts as a relay between the mobile users and another stationary base station Figure 2(b), this approach decreases the blockage percentage, but still, the resulting interference from a neighboring cell is left unresolved.

The last approach which we used and utilized in our study is using the UAVs as a backhauling hub connected to the core network Figure 2(c); our contribution to this approach is using the UAV as a self-backhauling

in a multi-hoping and multi-hierarchical way to deliver the transmitted traffic by the mobile users through the connected stationary base station (small, macro or micro cells) to and from the corresponding wired fiber core network (F-BS). Using the UAV as S-BS is a promising solution to solve many of the facing problems such as reducing blockage and interference. Still, a new number of challenges could appear especially those related to the UAVs. An example of these challenges is the battery limitation capacity. To overcome these challenges, we are proposing a hybrid transmitting approach by utilizing FSO and RF for dynamically medium selection for mobile user traffic transmission.
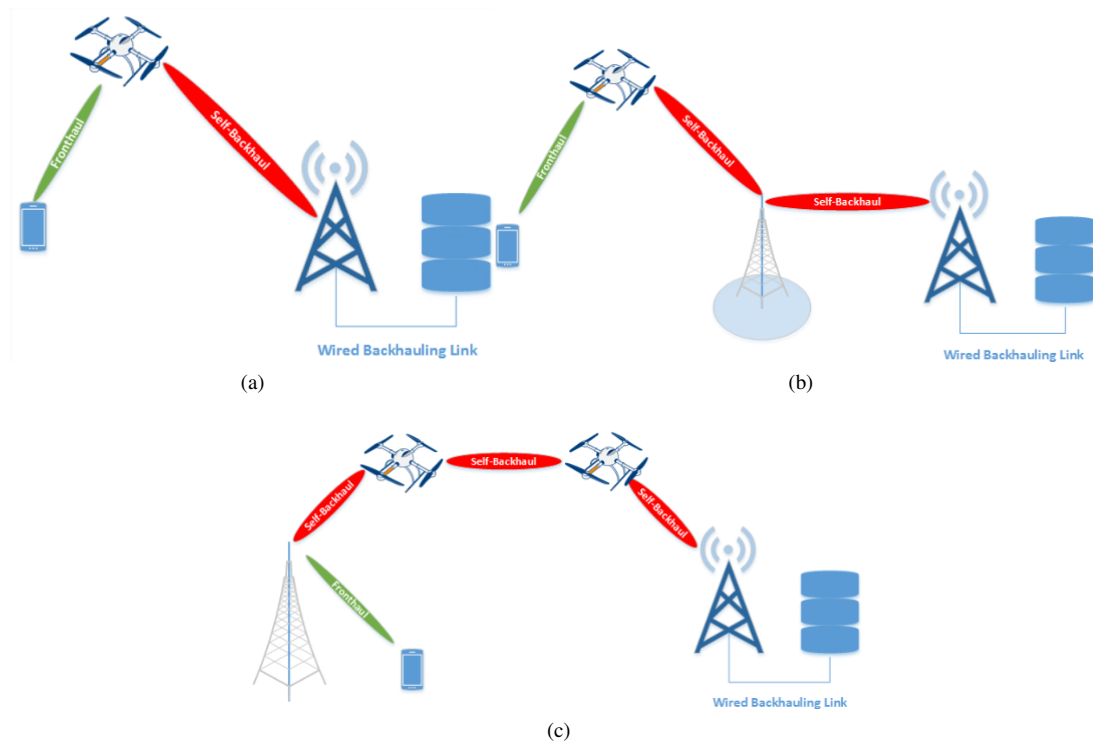

Figure 2. UAV as BS approaches (a) UAV as normal base station, (b) UAV as front hauling, and (c) UAV as backhauling

2.4. Hybrid FSO/RF communication medium

During the last years, the researcher shows that using FSO as a communication medium has a great potential and promising solution for many RF common challenges. The researcher in this area defines FSO as a LOS technology that uses a light-emitting diode (LED) or laser as a communication medium to provide a data rate in Gbps. The transmission of this optical communication is done in the free space as the term describes it (free space optical).

Based on the previous studies, FSO can provide a data rate up to 10 Gbps [10] without any need for any wiring solution (e.g., fiber-optic cabling) or spectrum licensing like radio frequency bands. As a benefit over the normal wiring fiber optics, FSO has less installation cost, maintenance cost, more flexibility, and better bandwidth efficiency since the light travels in glass (fiber optical cable) is slower than traveling in the free space. So we can fairly say that the FSO can transmit the data, voice, and video at the speed of light.

To utilize the FSO technology in telecommunications, we need three types of components, a transmitter, a medium, and a receiver. The first component is the transmitter, which is used to modulate and transmit the optical signal. The second component is the medium channel (free space), which carries the signal (this eventually suffers from signal attenuation resulting from the weather turbulence such as fog, haze, cloud, temperature, and rain). The last component is the receiver, which responsible to re-modulate the transmitted signal. One of the main advantages of using FSO (in addition to the great bandwidth) is the long transmission distance which reaching up to 5 km (in some circumstances, this distance could reach up to 12 km) comparing to the mm-Wave, which is not effective for distances exceed 150 meters. Also, the needed consumption power for

the transmission (which is a critical point in this research as we utilize UAVs as a flying base station with a relatively limited battery capacity) in the mm-Wave is higher than the FSO.

2.5.   Literature review

One of the newest techniques using with mm-Wave is the self-backhauling, which optimize the network usage and increase its efficiency. These techniques are proven to be an NP-hard problem in its simplest form without considering the interference and the mobility nature of the network [1], [11]. Unfortunately, this could work by simplifying and relaxing the problem by adding some assumptions to get non-NP-hard formulations [2], [11], or looking for heuristics [12] to simplify the problem constraints to build an incomplete or non-optimal solution to the mentioned problem [1]. Some of these assumptions and constraints simplification are the interference-free assumption in [1], [13] to find a mathematically tractable goals function. In reality, the mm-Wave networks are suffering from interference because of the deficiency of it is beamforming [9], [14] as wells as the first and second-order reflections especially inside the crowded cities [2], [8].

Besides that, in [1]–[3], [13]–[15] are assuming that there will be a fully-backlogged queue without considering the change of the traffic or the imbalance across the different segment inside the network, which could cause bottlenecks that decrease the performance, exhausting the resources and resulting in QoS degradation. Moreover, most of the proposed solutions are trying to maximize the throughput [1], [2], [11]–[13] without considering the latency in the backhaul links as an important factor. Because of the critical need for adaptability in these systems, most of the research focused on how to mitigate the resulting link outages from the beam misalignment due to the user mobility or links blockage [16]–[18]. Some authors like [16], [17] and [19], [20] proposed algorithms to predict the blockages and select the best alignment of the beams by analyzing users' mobility [16], [17]–[20].

Yuan *et al.* [1] tried to solve the route selection and scheduling problem as a linear programming problem to find the optimal throughput using the matching theory; Yuan *et al.* in [1] relaxed their problem by eliminating the interference factor. Till now, and based on our research and analyzing a lot of prior works, most of them do not take into account the interference, latency, first/second reflection, blockage, and changing of the traffic load in the same study. Moreover, many authors did not provide adaptability and robustness as a feature inside their solution while using dynamics networks, leading to link failures, frequent and unexpected changes in the traffic and channel fluctuations. Such issues make the network need to recompute the overall solution and select a new route, and rescheduling the traffic accordingly in case of any change. The work of [4] is the closest to our model, where the authors eliminate the interference-free assumption and take into account the latency, interference, and traffic load and manage the adaptability nature and robustness networks dynamic such as link failure, traffic variation and channel fluctuations. In addition, the authors focused on the solution (solution-oriented modeling) rather than focusing on the root of the problem (causal modeling), where they focus on reducing the major impact variables. They come with so-called symptom-based modeling in which they formulate the problem based on the symptom instead of what caused them. But in their solution, they are not trying to focus on solving the blockage which could introduce more interference. For their learning agent, they intended to use a greedy-based algorithm to return the optimal value. In contrast, this algorithm returns an optimal value but sometimes could go in an infinite loop.

3.   PROPOSED SOLUTION

The solution we are proposing is a variation of the scalable and robust self-backhauling solution for highly dynamic millimeter-wave networks (SCAROS) algorithm [4], in which we replace RF-BSs with high altitude S-BSs through the use of UAVs. Reductions in the blockage percentile and the interference probability are expected through the implementation of our proposed solution. We also adapt the data transmission medium to be highly dynamic and robust by accommodating the FSO technology based on the measured environment situation, as well as the regular RF communication. Our proposed solution consists of two types of multi-level UAV S-BS cellular network base-stations, i) Fiber-BS acting as backhauling base stations (F-BS) and ii) UAV-BS acting as self-backhauling base stations (S-BS).

F-BS is a regular stationary backhauling tower connected to the core network through a dedicated fiber-optic link. On the other hand, S-BS is a UAV-based self-backhauling base-stations that communicates with the F-BS through multi-hoping wireless links. These links could be either FSO or RF link based on the measured bit error rate (BER) value between any two hops. A graphical representation of the proposed solution is provided in Figure 3. Each of these base-stations is equipped with an FSO interface in addition to the regular

RF interface. In the proposed solution, we are assuming that all RF communication is done using the same RF bands [21].
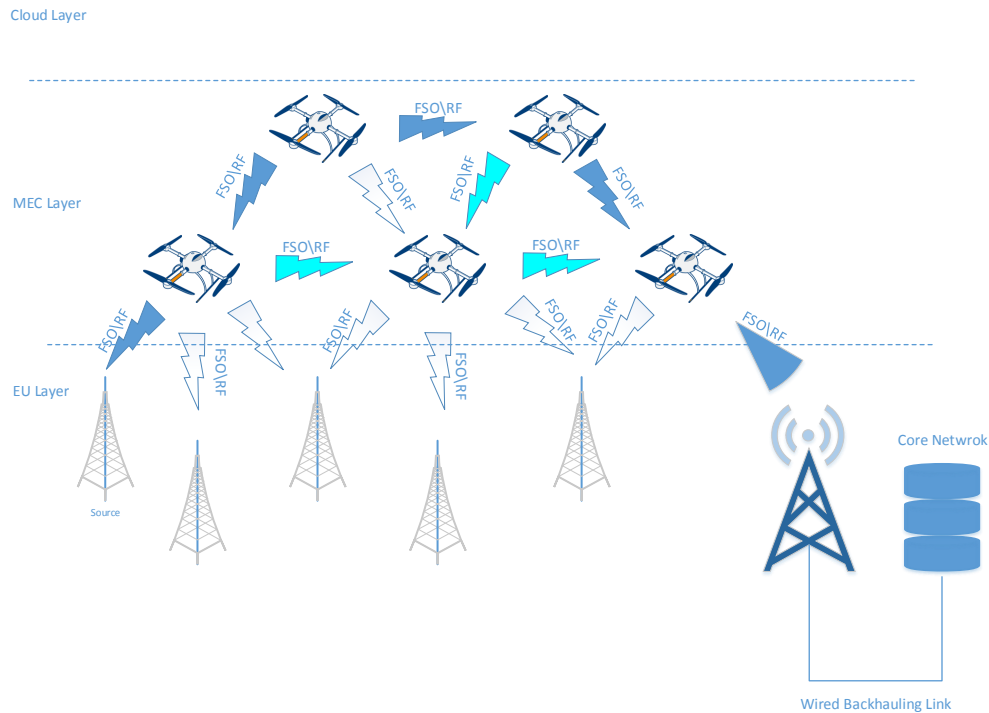

Figure 3. Self-backhauled mm-Wave UAV based cellular networks

To have an efficient communication system, both the allocation of time-slots and the route selection issues have to be addressed. Regarding the time-slotting issues, we are assuming that all time slots within our system have equal duration. Every time slot within it is denoted by a time index (T), where T is between 1 and a maximum value (t). As for the routing issue, we defined it for time slot t as $X_t \in X$, where X represents all the feasible route selection and scheduling solutions. Specifically, X_t is a $N_{BS} \times N_{BS}$ as (1) where N_{BS} is the number of available S-BSs.

$$X = \begin{pmatrix} 0 & x_{1,2}^{(t)} & \cdots & x_{1,N_{BS}}^{(t)} \\ x_{2,1}^{(t)} & 0 & \cdots & x_{2,N_{BS}}^{(t)} \\ \vdots & \vdots & \ddots & \vdots \\ x_{N_{BS},1}^{(t)} & x_{N_{BS},2}^{(t)} & \cdots & 0 \end{pmatrix}, \tag{1}$$

where $X_{n,m}^{(t)} \in \{-1, 0, 1\}$. At the beginning, we determine whether the link (n,m) between the two UAV hopes n and m (where $n \neq m$), is activated in time slot t. Then mark each hop based on the communication direction as in Table 2.

Table 2. Link states

Value	Link status
-1	n Rx, m Tx (n receives data from m)
0	Link is not activated
1	n Tx, m Rx (n transmits data to m)

Our aim here is to select the best route and scheduling solution with minimal end-to-end latency and BER; we can compute it as (2):

$$L = \frac{1}{N_{BS}} \sum_{n=1}^{N_{BS}} T_n(X),\qquad(2)$$

where L is the end-to-end latency measured in milliseconds (ms), while $T_n(X)$ is the resulting end-to-end measured in S-BS n when selecting the proper route and schedule it. This function is a stochastic function that depends on the factors: i) location of the UAV as a S-BS, ii) interference, iii) dynamics of the queue, and iv) user mobility.

Regarding the UAV location and for the sake of maintaining a better line of sight to increase the available communication bandwidth and downloads, each UAV is equipped with a GPS tracker that updates its location in a decentralized manner using a semi-distributed approach. Also, for the resulting interference and to minimize it, our proposed solution is utilizing the UAV to act as a flying S-BS with a reasonably high altitude. Adapting the UAV as an S-BS could reduce the expected interference to the lowest possible value due to its high altitude.

3.1.   INUSH algorithm

Due to the high dimensionality of the routing and scheduling problem, the innovative UAV self-backhauling hybrid solution using RF/FSO system for 5G networks and beyond INUSH algorithm optimizes the transmission with capabilities and enhancement to communicate over multiple mediums and devices, where RF towers operated as a front-backhauling only, while the multi-hoping path is introduced via UAV S-BSs. These UAV S-BSs are equipped with RF and FSO communication capabilities. The decision of which of the available mediums to select is based on predefined factors and the measurement between every two consecutive hopes.

For this kind of problems, dynamic programming techniques are used [22]. However, since we are dealing with a self-backhauling problem with recognized high dimensionality, such techniques are not a practical solution. To overcome these issues, we propose the INUSH algorithm, which is a reinforcement self-learning algorithm that aims at minimizing the end-to-end latency while increasing the available throughput for everyday users.

3.2.   Semi-distributed approach

We are using a semi-distributed approach in our proposed solution; Figure 4 shows the high-level architecture. The proposed architecture is designed to provide scalability and handle the increasing numbers of UAVs as an S-BSs and at the same time enhance the performance of the INUSH algorithm by reducing the time required to select the best available route with a proper propagation media. Figure 4 shows that every UAV S-BS is associated with a learning agent. Every learning agent is responsible for predicting the needed time to reach the F-BS based on recorded data from previously transmitted packets. The optimal route can then be calculated by taking into consideration weather turbulence, pointing error fading, and timing information collected by the learning agent.

The proposed semi-distributed learning approach is proven to remove the limiting factors of the number of used UAV as S-BSs and reducing the queuing time [4]. For the route selection process and the proposed algorithm, it is done in three stages, each stage runs according to a predefined algorithm and functions and runs in a specific order. First, the learning agent will call the INUSH algorithm which will invoke the synchronization control algorithm followed by the medium propagation selection algorithm.

3.3.   INUSH algorithm

In this section, we are giving a detailed discussion of the main INUSH outlined in algorithm 1, which intends to be invoked by each learning agent. First, every learning agent is initializing the learning parameters at (line 1). At (line 3), for each time slot, the algorithm observes the network hops states, collects, and registers them. At (line 5), the algorithm determines the available actions. Afterward, every learning agent selects the optimal route using the e-greedy policy (line 6). Next, The result or action provided by the learning agent is forwarded as an input to the synchronization control algorithm (line 8). Finally, the output is forwarded to the media propagation algorithm for final evaluating.
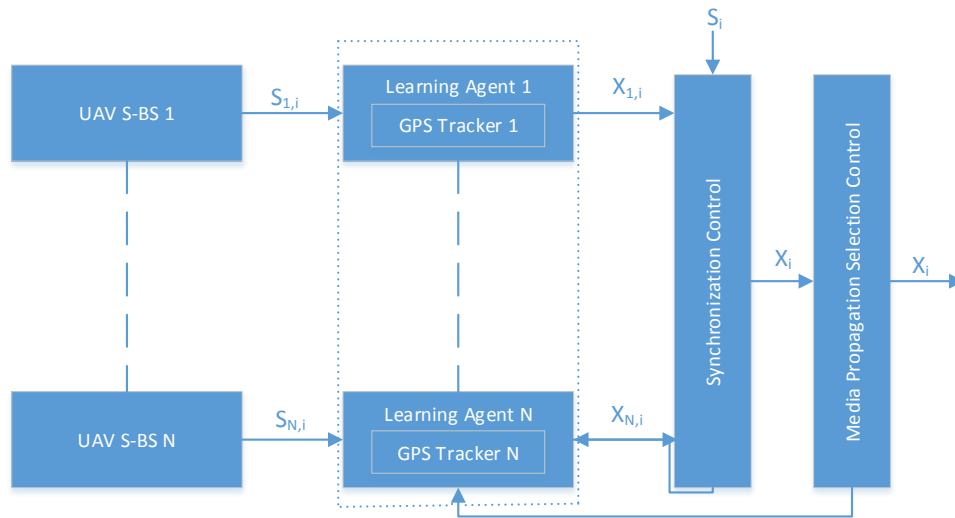
Figure 4. High-level architecture of the semi-distributed learning approach

---

Algorithm 1 INUSH algorithm

1: initialize α_n, ϵ_n at every equipped self-learning agent
2: **for** every $T = 1, ::: , t$ **do**
3:     measure state S_t
4:     **for** every learning agent $n = 1, ::: , N_{BS}$ **do**
5:         measure $S_{n,t}$ and find available actions
6:         select $x_n \in X_n$ using ϵ-greedy
7:     **end for**
8:     Invoke Synchronization Control Algorithm. Alg 2
9:     Invoke Medium Propagation Control Algorithm. Alg 3
10:    Apply X_t and measure the reward based on the target neighboring UAV_m TRx time and its estimates E-to-E latency
11:    Update E-to-E latency to its expected value in each time slot
12: **end for**
13: Exit

3.4. Synchronization control algorithm

Since the proposed solution uses a semi-distribution technique, any taken decision by any of the learning agents may conflict with the other agent's decisions (e.g., two or more UAV S-BSs attempting to transmit data to the same UAV S-BS at the same time). To overcome this problem, our solution proposes another algorithm called the synchronization control algorithm. The aim of this algorithm is synchronizing the overall route selection mechanism and make sure that there is no transmission conflict between the UAVs, as well as reducing the interference. The pseudocode of the synchronization control algorithm is defined in algorithm 2. Table 3 summarizes the used parameters within this algorithm along with the meaning and purposes for each of them.

From Table 3, we can see that at the beginning, the algorithm collects the current states for every hop in the network s_t, the action selected by each learning agent x_n, the selected route X_t as well as the interfering links I_{n-m} (n transmits to m) that being transmitting over. This algorithm will use the information in Table 3 to run and return its result through three specific phases (loops) to ensure that the selected route is feasible, assignable, and applicable to be used by the asking UAV S-BSs. In the first phase or loop, the proposed solution eliminates any simultaneous activation of the selected route's interfering links. After that, the second phase/loop starts, which in turn checks and makes sure that no two or more UAVs are attempting to transmit to the same UAV S-BS. Finally, at the third and last phase, the proposed algorithm ensures that for every transmitting UAV, the target neighboring UAV S-BS is in receiving mode.

Algorithm 2 Synchronization control algorithm

1: check s_t and x_n for n = 1; ::::;N_{BS}
2: calculate X_t
3: **for** $n = 1, ..., N_{BS}$ **do**
4:    **if** $I_{n-m} \neq 0$ **then**
5:       lookout for all the Trx UAV BS $l \in I_{n,m}$ knowing that
        $\{S_{l,i} = max(S_{k,i})|(k = 1, ::::, N_{BS}) \cup (k \in I_{n,m}).\}$
6:       Deactivate all the other Trx UAV BS $k \neg l, k; l \in I_{n,m}$
7:    **end if**
8: **end for**
9: **for** $m = 1, ::::, N_{BS}$ **do**
10:    **if** $\sum_{n=1}^{N_{BS}} X_{n,m} > 1$ **then**
11:       Lookout for all the Trx UAV BS knowing that
        $\{S_{l,i} = max(S_{k,i})|(k = 1, ::::, N_{BS}) \cup (X_{k,m} = 1\}$
12:       Deactivate all the other Trx UAV BS $k \neg l$
13:    **end if**
14: **end for**
15: **for** $n = 1, ::::, N_{BS}$ **do**
16:    **if** $x_{n-m} \neg x_{m,n}$ **then**
17:       **if** $s_{n,i} \geq s_{m,i}$ **then**
18:          Operate UAV BS m as a receiver BS
19:       **else**
20:          Operate UAV BS n as a receiver BS
21:       **end if**
22:    **end if**
23: **end for**
24: Exit

Table 3. Synchronization control algorithm parameters

Parameter	Description
s_t	Current state of the network
x_n	Action selected by learning agent
X_t	Corresponding route selection
I_{n-m}	Interfering links (n transmits to m)
$\sum_{n=1}^{N_{BS}} X_{n,m} > 1$	two or more UAV S-BS intended to Trx to the same UAV
$x_{n-m} \neg x_{m,n}$	make sure that every TRx UAV, the targeting neighbor UAV is in Rx mode

3.5. Medium propagation selection algorithm

Previous experiments and simulations show the promising advantage of hybrid systems over traditional RF-based communication [23]. This algorithm aims to check every proposed route received from every learning agent for the overall bit error rate (BER) to validate the possibility of using FSO as a propagation medium or keeping the RF medium in use. In algorithm 3, we are assuming that the default and worst-case is using the RF as a propagation medium (line 1). At (line 2 and 3), the INUSH algorithm measure the atmospheric turbulence fading (I_a) as well as the pointing error fading (I_p) for every link between each UAV S-SB and the next UAV S-BS along the selected route.

Algorithm 3 Medium propagation control algorithm

1: consider using RF by default
2: compute the atmospheric turbulence fading (T_a) at every UAV-UAV path
3: compute the pointing error fading (T_p) at every UAV-UAV path
4: **while** path not reach final backhual **do**
5:    compute BER_{rf} using RF between UAV_t and UAV_{t+1}
6:    compute BER_{fso} using FSO between UAV_t and UAV_{t+1}
7:    **if** $BER_{fso} \leq BER_{rf}$ **then**
8:       Switch UAV $S - BS_t$ Tx to FSO mode
9:       Switch UAV $S - BS_{t+1}$ Rx to FSO mode
10:    **else**
11:       Switch UAV $S - BS_t$ Tx to RF mode
12:       Switch UAV $S - BS_{t+1}$ Rx to RF mode
13:    **end if**
14: **end while**
15: Exit

Afterword and at (line 5), the INUSH algorithm will calculate the RF BER_{rf} using the SNR value from the received signal strength indicator (RSSI) considering that the RF medium being used between the two hops being examined. Similarly, at (line 6), the INUSH algorithm will measure FSO BER_{fso} using the SNR value from the RSSI, the current weather, and the fading considering that the FSO medium is used between the two hops that being examined. Going ahead to (line 7), the INUSH algorithm will start to compare the calculated values of the BER_{fso} and BER_{rf}. If the BER_{fso} is less than or equal to the calculated BER_{rf}, then the FSO will be selected as a transmission medium over the RF. Simultaneously, the corresponding UAV $S\text{-}BS_i$ will be activated as FSO transmitting hope, and UAV $S\text{-}BS_{i+1}$ will be activated as FSO receiving hope (Line 8 and 9). If not and similarly, the algorithm will switch the corresponding UAV $S\text{-}BS_i$ to be transmitting hope using RF medium and UAV $S\text{-}BS_{i+1}$ receiving hope to RF medium as well (Line 11 and 12). The same process is repeated between every two hops in the selected route, pair by pair until reaching the final hope.

3.5.1. Atmospheric turbulence model

In FSO, the signal is affected by two significant factors: the atmospheric turbulence fading $I = I_a$ and the pointing error fading $I = I_p$. Because of these factors, the optical signal intensity fluctuations at the receiver side computed as $I = I_a I_p$ [24]. The INUSH algorithm determines which propagation media to use by finding the intensity fluctuations between each two UAV S-BSs in the selected path. To compute the optical signal intensity fluctuations related to the FSO channel, we are assuming the same as [23] where the Gamma–Gamma distribution model is used for the link fading modeling.

Accordingly, we can compute the probability density function (PDF) using (3):

$$f_{Ia}(I_a) = \frac{(\alpha\beta)^{\frac{\alpha+\beta}{2}} I_a^{-1}}{\Gamma(\alpha)\,\Gamma(\beta)} G_{2,0}^{0,2}(\alpha\beta I_a | \alpha, \beta) \tag{3}$$

where G represents the Meijer-G function and Γ is the gamma function. In contrast, α and β are representing the large-scale and small-scale cells in the atmosphere.

For α and β parameters, it is computed by (4) and (5),

$$\alpha = \left[exp\left(\frac{0.49\sigma_l^2}{(1 + 1.11\sigma_l^{12/5})^{7/6}} \right) - 1 \right]^{-1} \tag{4}$$

and

$$\beta = \left[exp\left(\frac{0.51\sigma_l^2}{(1 + 0.69\sigma_l^{12/5})^{5/6}} \right) - 1 \right]^{-1} \tag{5}$$

where $\sigma_l^2 = 1.23 C_n^2 (2\pi/\lambda)^{7/6} Z^{11/6}$ is the log radiance variance, and Z is the distance between sender and receiver, while C_n^2 is the index of the refraction structure parameter (introduced by Kolmogorov), that constant for the horizontal link [25].

3.5.2. Pointing error fading

Relaying on the research done by Jurado-Navas *et al.* [26], the probability density function of I_p is computed by (6),

$$f_{Ip}(I_p) = \frac{\vartheta^2}{A_0^{\vartheta^2}} I_P^{\vartheta^2 - 1}, \;\; 0 \le I_P \le A_0 \tag{6}$$

where A_0 is the fraction of the collected power when $r = 0$; r and $\omega_z = \omega[1 + \varepsilon(\lambda Z/\pi\omega_0^2)^2]^{1/2}$ are the hole radius and the beam waist at distance Z.

The most important parameter in (6) is $\vartheta \triangleq \varepsilon_{zeq}/(2\sigma_s)$ which is the relative ratio between the beam radius and the pointing error standard deviation. In the same manner, if $\vartheta = 1$, then the pointing error is too high. Hence, if ϑ is going high, the pointing error itself will go down while (If $\vartheta \to \infty$, the pointing error becomes negligible). For the sake of minimizing the pointing error fading, and as we mentioned before; each UAV S-BS will be equipped with a GPS tracker, which allows the UAV S-BSs to update their location in the corresponding locations manager. From the corresponding locations manager, every UAV will know where the other UAVs' location will be at any time instance and align its FSO receivers or transmitters accordingly.

3.5.3. Mixing fading parameters

In our solution, we are assuming that all links in the selected path or route are independent of each other since the date transmission between every two hops in the same route does not depend on any previous hops at the same route, and since all the previous equations that used to calculate the end-to-end relation and measure the SNR value to calculate the BER between the different hops in the selected route is a little bit complicated, so we are going to use a simplified expression (7),

$$\lambda_{fso} = \frac{\lambda_1 \lambda_2}{\lambda_1 + \lambda_2 + 1} \sim min(\lambda_1, \lambda_2) \tag{7}$$

where λ_1 and λ_2 is the BER of the FSO and RF in the selected path. Using the same approach, if λ_3 and λ_4 is the BER of FSO and RF links, we can compute the BER of that link (P_2) as (8):

$$\lambda_{rf} = \frac{\lambda_3 \lambda_4}{\lambda_3 + \lambda_4 + 1} \sim min(\lambda_3, \lambda_4) \tag{8}$$

on the next hop where the next UAV S-SBs is intended to receive the signal, the propagation media selection algorithm will select the link with the lowest BER $\lambda_{SC} = max(\lambda_{fso}, \lambda_{rf})$.

4. RESULTS AND DISCUSSION

4.1. INUSH complexity analysis

In this section, we analyze the complexity of the proposed INUSH algorithm for one iteration. We considered the measured network size, where the number of UAV S-BSs is (N_{BS}) is the deciding factor in the network. We will also show how the INUSH algorithm's complexity is significantly less than the traditional reinforcement learning algorithms such as SARSA [22] and SCAROS [4].

To determine the big-O complexity of the INUSH algorithm, we will begin by calculating the complexity of the synchronization control and media propagation control algorithms. Then, the complexity for both algorithms will be combined to build the total INUSH algorithm complexity. We will start by analyzing the synchronization control algorithm. As we discussed before, it consists of three phases, and each phase is composed of one for-loop, which is responsible for checking the status and the selected action of the neighboring hops. All three loops are running independently and in sequence. The worst-case complexity for all the phases is equal to O($3N_{BS}^2$), which is equal to O(N_{BS}^2) since these operations have to find the maximum values of the state of all available S-BS which equivalent to O(N_{BS}). And as this keep repeating N_{BS} times, so the complexity for each phase is O(N_{BS}^2), and since there are three independent loops so the overall complexity remains O(N_{BS}^2)

Going to the medium propagation control function, it is clear that the most computationally extensive sequence is within the while statement(lines 4-14). This while statement represents the number of hops in the selected route, denoted by M_{BS}, so the overall complexity of the medium propagation control function is O($M_{BS} - 1$), which is the number links that the algorithm will examine until reaching the core network. Using the same approach, we will evaluate the complexity of the INUSH algorithm itself. We noticed that the most complicated operations performed inside the loop (lines 4-7) in which the synchronization and the media propagation functions were invoked. Hence, we are using the ϵ-greedy policy; the worst-case is finding the required action that leads to the minimum latency. The time complexity for this operation can go as O(N_{BS}), which is the same as ϵ-greed big-O complexity. Since the operation is run independently inside each learning agent, the complexity will remain the same.

Regarding synchronization control function and as discussed in the previous paragraph, it is growing up to O(N_{BS}^2). Now, for the media propagation selection function and similarly, as discussed before, it goes up to O(M_{BS}) in the worst case as well. Using the same analysis technique, Ortiz *et al.* [4] computed the complexity of Q-learning and SARSA algorithms. Comparing our proposed solution to their work, we can see that their complexities depend firmly on the network size $|\chi|$ due to the use of a centralized learning technique to solve the formulated problem. Therefore, as $\Pi_{n=1}^{N_{BS}} \gg N_{BS}^2 \times M_{BS}$, INUSH shows significantly smaller time complexity compared to the other learning schemes.

4.2. Reliability against weather turbulence

In this section, we are discussing the reliability and performance of our proposed solution under different weather turbulence conditions. During the simulation, and as this paper targets 5G and beyond networks,

we choose to do the simulation for sub-6 GHz frequencies. The aims of the performed simulation to give an insight into how the INUSH algorithm will work using these frequencie bands. For the used parameters in our simulation, Table 4 is listing them.

For the number of hops, our proposed solution was designed and evaluated for N number of hopes. For the sake of performing the simulation, we choose 20 as a value of N. The reason behinds this selection that the 20-hops may cover an area of $400\ m^2$ ($20 \times 20 = 400\ m^2$) in the case of approaching ultra-density deployment. Similarly in the medium density deployment, the covered area could reach up to 3-km ($150 \times 20 = 3000\ m^2$) and in sparse this value becomes 10-km ($500 \times 20 = 10000\ m^2$).

Table 4. Simulation parameters

Parameter	Value	Description
Noise floor	-90 dBm	RF noise floor
Number of Hops	0-20	Number of hops to reach the core
RF transmitted power	-10 dBm	RF transmitted power
	1-20 m	Distance in ultar-density deployment
Distance between hops	1-150 m	The HPC2N Seth log
	1-500 m	Distance in sparse deployment

Regarding the SNR for every link, we can calculated as (9),

$$SNR = Received_Power - Noise_Floor \qquad (9)$$

while the received power calculated using Friis transmission as (10),

$$Prx = Ptx + Gtx + Grx + 20Log10(Lamda/(4PiDr)) \qquad (10)$$

where Prx is the received power, Ptx is the transmitter power, Gtx is the transmitter gain, Grx is the receiver gain, $Lamda$ is the wave length, and Dr is the distance between the transmitter and the receiver.

Going further in this discussion, we performed the simulation using different weather turbulence conditions. Table 5 summarizes the considered weather conditions along with their related parameters. For the sake of the performed experiment more realistic, we set the weather fluctuation percentage to be $\pm$ 10% between every hop and the next one.
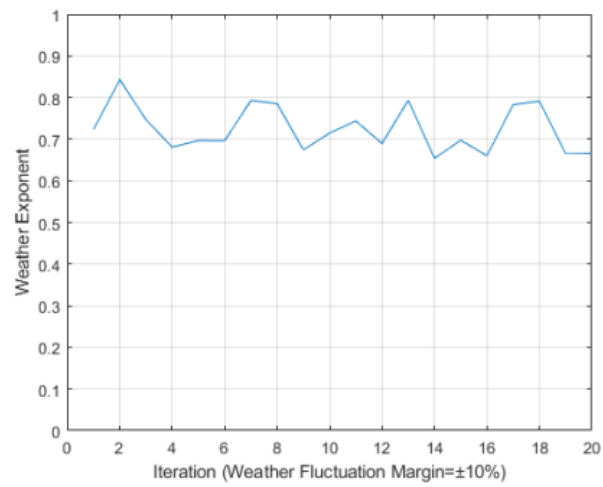
Table 5. Weather conditions

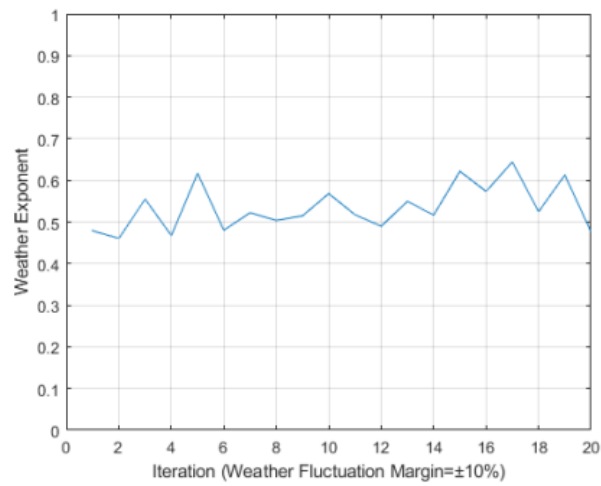| Weather Turbulence	Description
Good weather	Visual clearance is around 75%
Moderate weather	Visual clearance is around 55%
Bad weather	Visual clearance is around 25%

We considered different values to simulate the different weather conditions in our experiments; Figure 5 shows these values. To add more realism, we set the weather fluctuation factor to $\pm$ 10% between every two hops. We choose 3-different values as the following, Figure 5(a) shows the expected simulation values during summer where the visibility clearance is around 75%. For the autumn and spring seasons, Figure 5(b) simulates them with around 55% visibility clearance, and finally, Figure 5(c) simulates the winter with around 25% visibility clearance. During this simulation, we took into consideration the distance between different hops as a parameter. This parameter has a significant effect on the transmission for both the RF and FSO communication and the weather fluctuation that we mentioned before, which has a considerable effect on the FSO transmission.

4.2.1. INUSH simulation summary

Subsection 4.2.2., 4.2.3., and 4.2.4., shows the reliability against different weather turbulence. It represented one experiment of 20 hops under 25% as bad weather, 55% as moderate weather, and 75% as good weather conditions. We repeated the experiment of 20 hops for 100 times and summarized the average BER at different weather and densities in Table 6. The selection ratio between FSO/RF is presented in the rightmost column (H-Ratio).

(a)

(b)
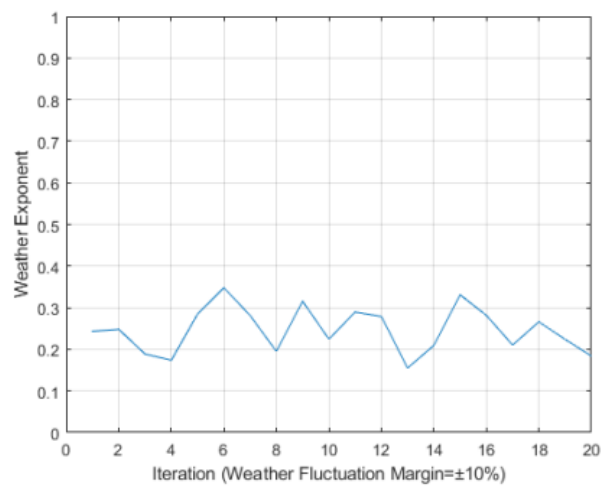
(c)

Figure 5. Weather turbulence fluctuation (a) good weather turbulence, (b) typical weather turbulence, and
(c) bad weather turbulence

Table 6. BER comparison between different weather conditions and distances on 6 GHz

Visibility	Deployment	RF Path BER	FSO Path BER	Hybrid Path BER	H-Ratio (RF:FSO)
25%	Dense	1.27×10^{-5}	2.90×10^{-02}	1.21×10^{-5}	0.99 : 0.01
	Medium density	4.34×10^{-2}	2.77×10^{-02}	6.90×10^{-3}	0.54 : 0.46
	Sparse	2.42×10^{-1}	3.21×10^{-02}	2.14×10^{-2}	0.22 : 0.78
45%	Dense	7.48×10^{-6}	1.41×10^{-6}	1.34×10^{-7}	0.73 : 0.27
	Medium density	4.44×10^{-2}	1.27×10^{-6}	1.01×10^{-6}	0.16 : 0.84
	Sparse	2.32×10^{-1}	1.38×10^{-6}	1.24×10^{-6}	0.06 : 0.94
55%	Dense	1.02×10^{-5}	9.06×10^{-9}	3.54×10^{-9}	0.40 : 0.60
	Medium density	4.14×10^{-2}	8.82×10^{-9}	7.89×10^{-9}	0.07 : 0.93
	Sparse	2.38×10^{-1}	9.40×10^{-9}	9.14×10^{-9}	0.02 : 0.98
75%	Dense	6.54×10^{-6}	4.11×10^{-13}	4.10×10^{-13}	0.00 : 1.00
	Medium density	4.37×10^{-2}	4.04×10^{-13}	4.04×10^{-13}	0.00 : 1.00
	Sparse	2.27×10^{-1}	3.78×10^{-13}	3.78×10^{-13}	0.00 : 1.00

4.2.2. Reliability under good weather turbulence

As we mentioned before, good weather turbulence occurs when the visual clearance is around 75%. In our simulation, we assumed that it needs up to 20 hops to reach the backhauling base stations (F-BS). Our simulation is done using sub-6 GHz frequency bands.

Figure 6 shows how INUSH behaves under different network densities, namely sparse, medium density, and Dense Network using 6 GHz frequency bands. Figure 6(a) illustrates the communication behavior in a sparse network where the distances between any two hops in the selected route does not exceed 500 meters. Here we can see that our hybrid solution takes the same behavior as the FSO-Only solution, which meets our expectation as the visual clearance is around 75% which gives an advantage of using FSO communication. Using the same approach, Figure 6(b) shows the result in the medium-density networks, where the distances between any two hops are up to 150 meters. The same as Figure 6(a), our hybrid solution takes the same behavior as the FSO-Only solution. Finally, regarding Figure 6(c), it shows the result in the dense network deployment, where the distances between any two hops are not exceeding 20 meters. When comparing the BER between the three route types, RF-Only, FSO-Only, and hybrid route, we can notice, as in Figure 7, the BER is evaluated under different network densities; sparse in Figure 7(a), medium density in Figure 7(b), and dense in Figure 7(c). Since the weather condition is in its best condition, where the clearance is around 75%, the hybrid solution rely mainly on FSO links due to the lower BER, hence the same BER as the FSO-only solution in Figures 7(a)-(c).

## 4.2.3. Reliability under bad weather turbulence

After discussing the result under good weather turbulence, we will discuss INUSH's performance and behavior under bad weather turbulence. As we mentioned before, bad weather turbulence occurs when the environment visual clarity around 25% or less. For the number of hops, we will maintain the same assumption as before, which is up to 20 hops until reaching the corresponding F-BS. Figure 8 shows how our proposed algorithm behaves under different network densities: sparse, medium and dense network using 6 GHz frequency bands.

Figure 8(a) shows the communication behavior in sparse network deployment where the distances between any two hops are up to 500 meters. We can notice here that our INUSH hybrid solution takes better behavior comparing to both RF-Only and FSO-Only solutions. Using the same approach, Figure 8(b) shows the result for the medium density networks (distances between any two hops are up to 150 meters), The same as Figure 8(a), INUSH hybrid solution gives better BER values comparing to RF-Only and FSO-Only solutions. Finally, Figure 8(c) shows the result in dense network topology (distances between any two hops not more than 20 meters), which give the same behavior as the RF-Only solution due to the short communication range.

In Figure 9, we present the measured BER between these three route types (RF-only, FSO-only, and hybrid routes) in sparse deployment as in Figure 9(a), medium density as in Figure 9(b), and dense deployment as in Figure 9(c). And since we discuss the behavior under the bad weather (the visual clearance is around 25%), the INUSH hybrid solution will rely heavily on FSO-only when the network is sparse due to the high BER in RF in such condition as seen in Figure 9(a). When the network is densely deployed, RF channel will have a very low BER and the hybrid solution will rely on RF-only links as shown in Figure 9(c).
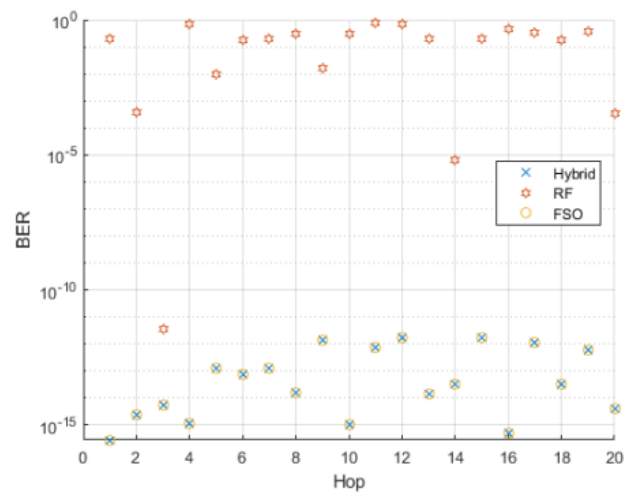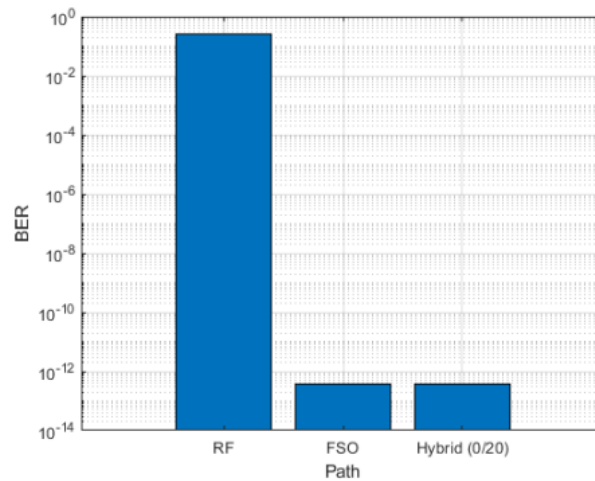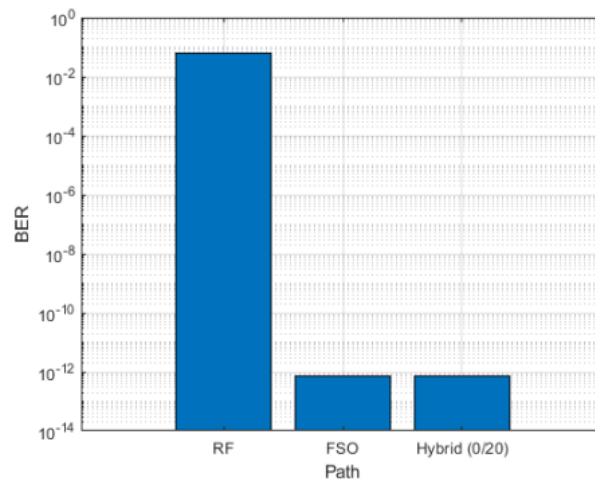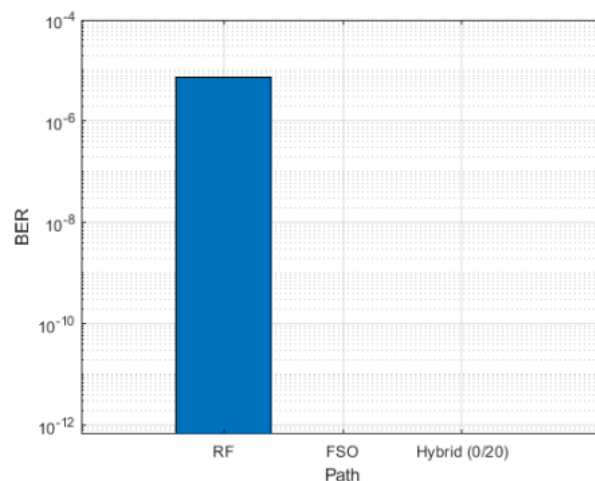
(a)
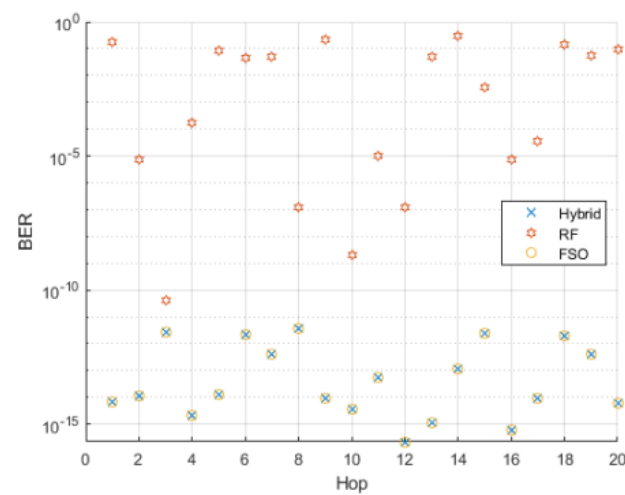
(b)
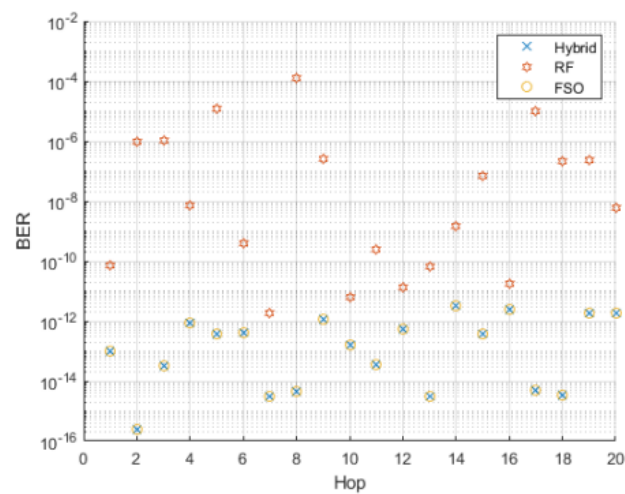
(c)

Figure 6. 6 GHz network density deployment comparison under good weather (a) sparse network, (b) medium density network, and (c) dense network
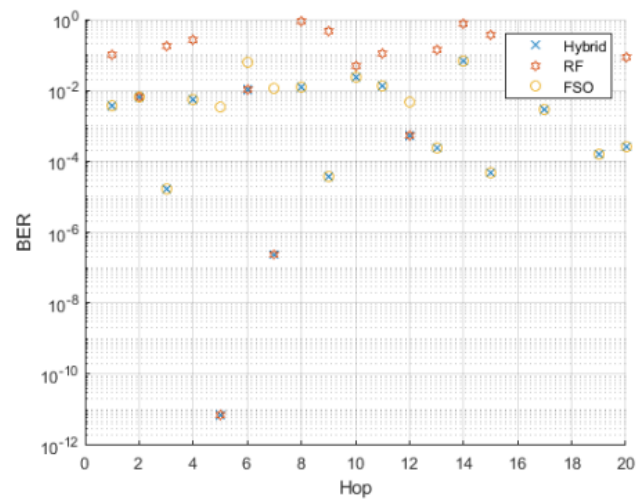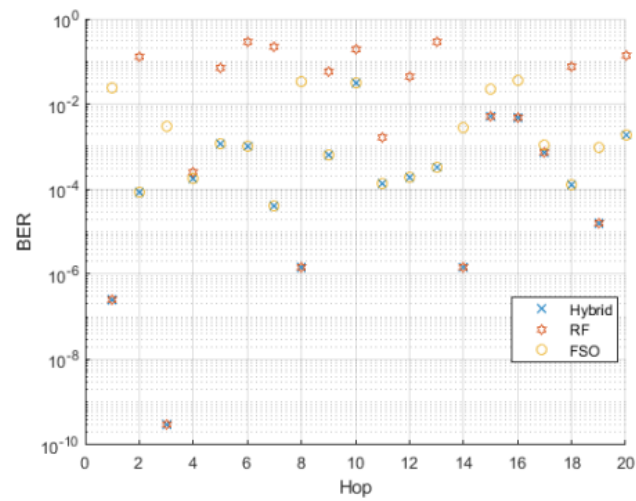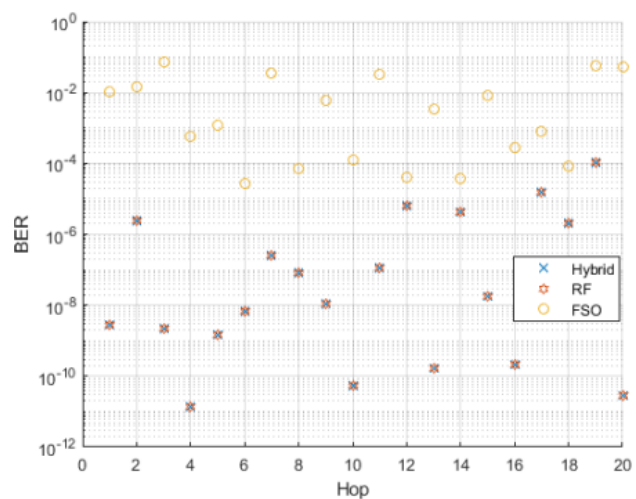
(a)

(b)

(c)

Figure 7. 6 GHz network density deployment BER comparison under good weather, the number in hybrid bar is the ratio between RF/FSO (a) sparse network BER, (b) medium density network BER, and (c) dense network BER

(a)

(b)

(c)

Figure 8. 6 GHz network density deployment comparison under bad weather (a) sparse network, (b) medium density network, and (c) dense network
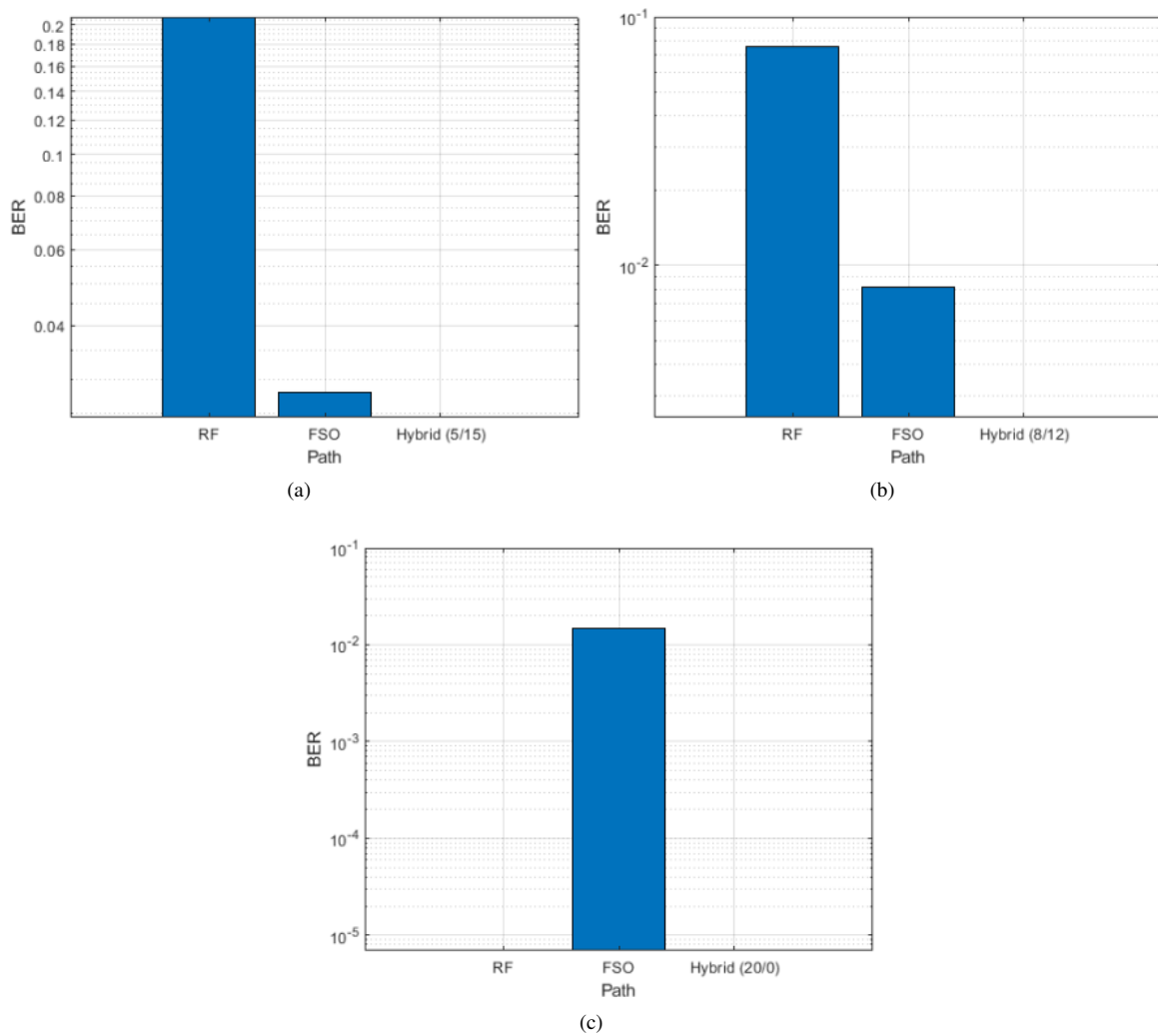
Figure 9. 6 GHz network density deployment BER comparison under bad weather, the number in hybrid bar is the ratio between RF/FSO (a) sparse network BER, (b) medium density network BER, and (c) dense network BER

4.2.4. Reliability under moderate weather turbulence

After discussing the extreme weather cases, which weather either in its best or worst condition, we will discuss the INUSH algorithm under average weather turbulence. In moderate weather turbulence, the visual clarity is 55%, representing the average during the year as it is present in almost two seasons (spring and autumn). As mentioned before, moderate weather turbulence occurs when the environment visual clarity around 55%.

In our experiment, we considered a light fluctuation in weather turbulence between every hop and next consecutive hop on the selected route. We maintain the same value we used in the previous simulation to be ±10% of the current weather condition at the last examined hop. Such fluctuation happened for many reasons such as temporary smoke or temporary blockage, even any type of FSO signal attenuation that could eventually affect receiving the FSO signal. For the number of hops, we maintained the same assumption as before, which is up to 20 hops until reaching the corresponding F-BS. Now we are going to discuss the result when using 6 GHz frequency; Figure 10 shows how our proposed algorithm behaves under the different network density using 6 GHz frequency bands.

Figure 10(a) shows the communication behavior under a sparse network deployment where the distances between any two hops are up to 500 meters. It is noticeable that the INUSH hybrid algorithm shows

almost the same behavior as the FSO-Only solution, and the reason behind that the mm-Wave communication range is relatively low. Using the same approach as in a sparse network, Figure 10(b) shows the obtained result in the medium-density networks (distances between any two hops are up to 150 meters). In this type of deployment, our INUSH hybrid algorithm took the same behavior as the FSO-Only. However, still, there are a small number of hops that decided to communicate over RF channels. Finally, Figure 10(c), shows the obtained result in the dense network deployment (distances between any two hops are not more than 20 meters). Here we can see that at some points, the solution decided to go over RF channels since the BER at that point is smaller than the FSO BER due to the short observed distance, which gives an advantage to the RF communication.
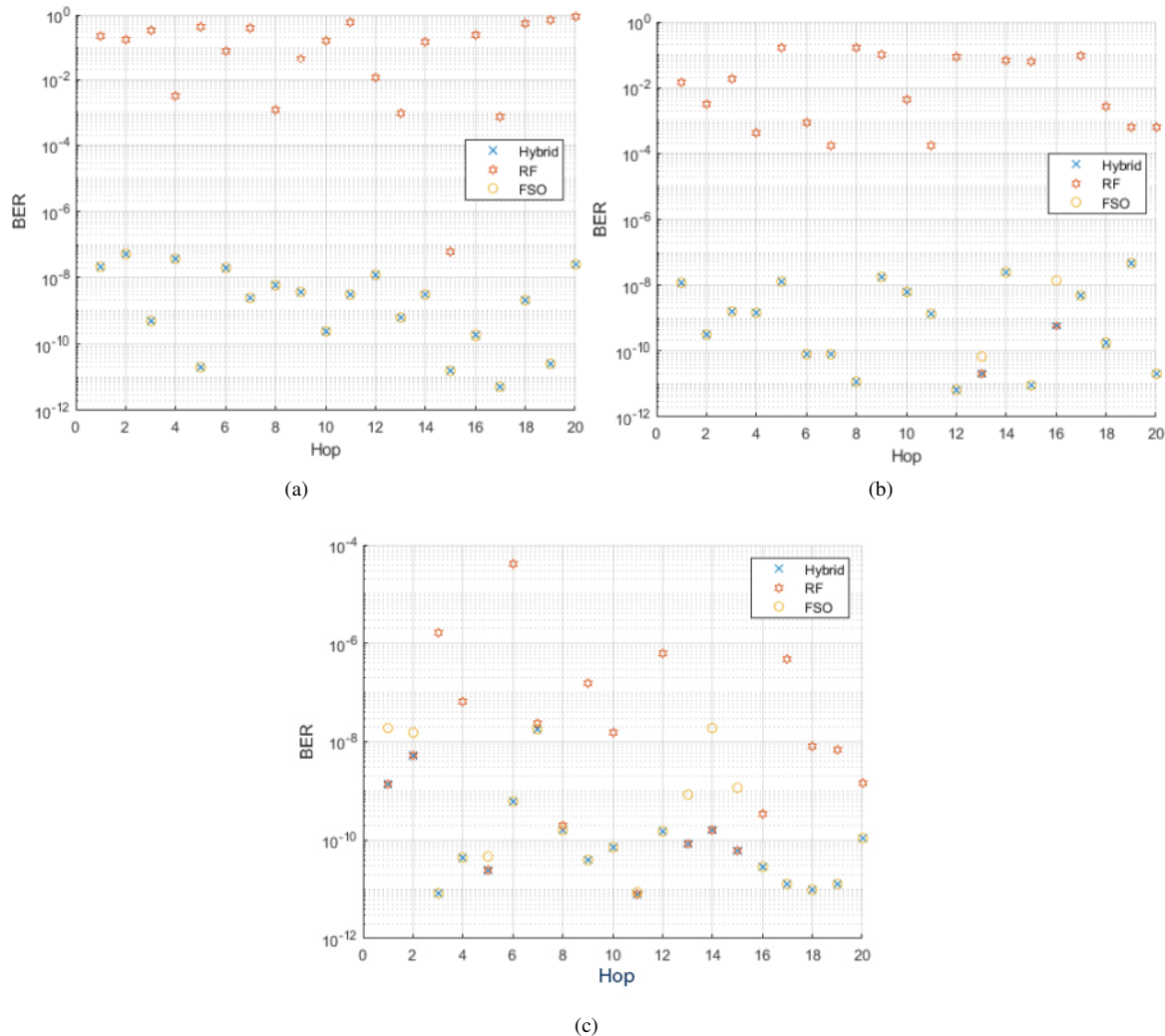

(a)

(b)

(c)

Figure 10. 6 GHz network density deployment comparison under moderate weather (a) sparse network, (b) medium density network, and (c) dense network

By comparing the BER between the three route types (RF-Only, FSO-Only, and Hybrid routes) in the different network densities, Figure 11 shows the differences between them. For example, Figure 11(a) represent the average BER in the sparse network and showing how the INUSH performed the same as FSO-Only techniques. Figure 11(b), comparing the obtained BER in the medium density network between RF, FSO, and our hybrid technique. We can notice that the result is better than both RF and FSO only solution since it chooses the lowest BER value between the RF and the FSO, resulting in better route performance Finally, Figure 11(c), shows the obtained BER in the dense network. We can see that it is much better in the hybrid solution than the RF and FSO only solutions since the hybrid solution chooses the lowest BER between the RF

and the FSO, resulting in better QoS. To clarify the obtained result, Table 7 give more details and summarization of Figure 11, which comparing our INUSH hybrid algorithm against RF-Only and FSO-Only solutions.
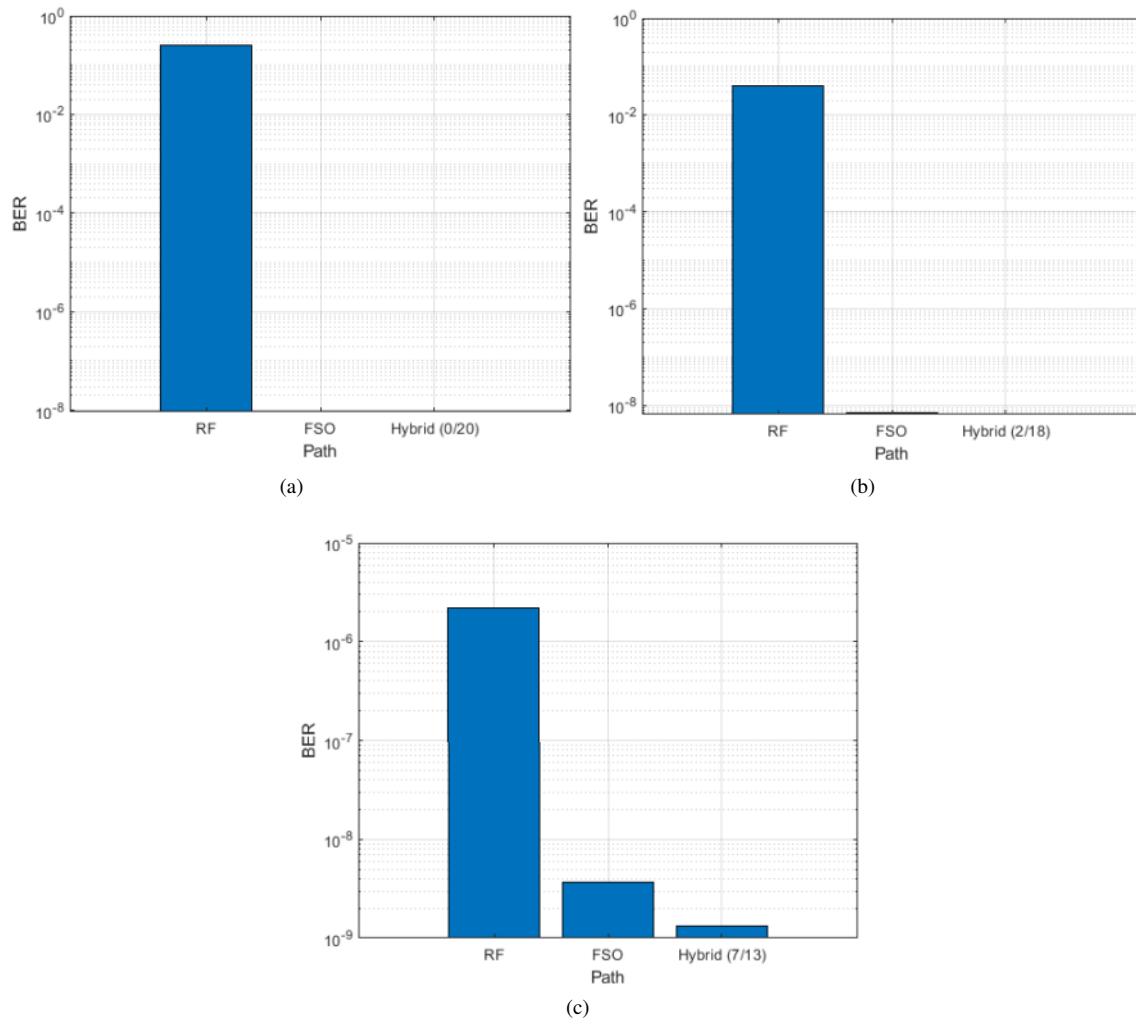

(a)

(b)

(c)

Figure 11. 6 GHz network density deployment BER comparison under moderate weather, the number in hybrid bar is the ratio between RF/FSO (a) sparse network BER, (b) medium density network BER, and (c) dense network BER

Table 7. Routes BER comparison based on network density

Route Type	Sparse	Medium Density	Dense
RF:FSO hops	0:20	2:18	7:13
RF BER	10^{-1}	$10^{-1.5}$	$10^{-5.5}$
FSO BER	10^{-8}	10^{-8}	$10^{-8.5}$
Hybrid BER	10^{-8}	10^{-9}	$10^{-8.9}$

4.3.   Robustness against load imbalance

In this part, we discuss the load-balancing in self-backhauling networks. Figure 12 shows how the load imbalance will affect the throughput. While Figure 13 shows the same for end-to-end latency. As we can see in Figure 12, INUSH shows significant throughput increases (up to 8-Gbps) compared to SCAROS, which is less than 8-Gbps and RT which is steady of almost 1.75-Gbps while MTFS with 3-Gbps INUSH algorithm takes the better values between the FSO and the RF. For end-to-end latency, as in Figure 13, INUSH shows a steady line with almost 0.055 seconds, while SCAROS shows a higher latency with 0.07 seconds. For RT, we

can see that it shows almost 0.08 seconds over the same period while MTFS increasingly shows high end-to-end latency with up to 0.25 seconds over the same period and the same as before; INUSH chooses the route with the smaller BER, which affects the overall performance.
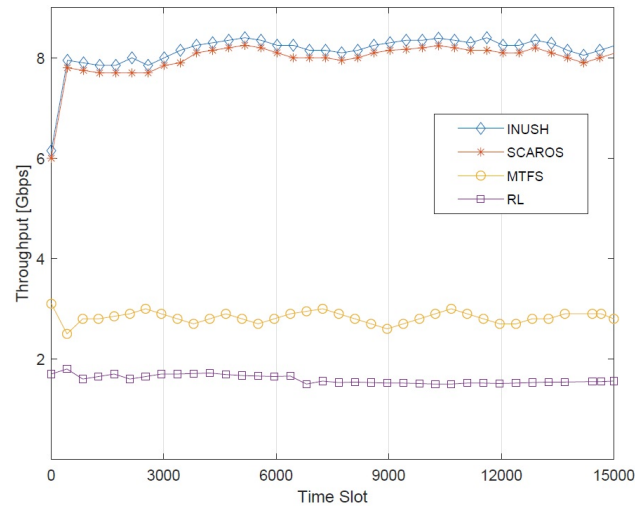

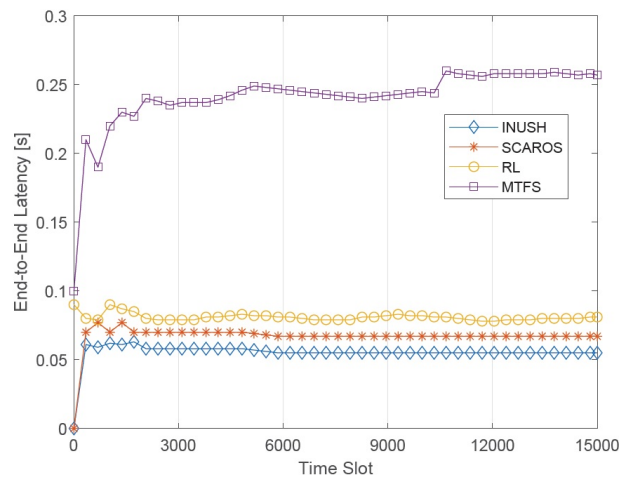Figure 12. Throughput comparison between different schemes

Figure 13. End-to-End latency comparison between different schemes

5. CONCLUSION

In this work, we presented a scalable and robust algorithm, INUSH, which depends on decentralized self-learning approach to find the optimal route in self-backhauled mm-Wave networks with a realistic network dynamics nature such as interference and mobility. Our proposed solution uses UAVs as self-backhauling base stations while keeping the standard stationary macro, micro, and small towers to provide front-backhauling functionality to the mobile users. Using this approach, we increased the available bandwidth, throughput, and data rate for normal mobile users because of utilizing the stationary base stations for them.

Since the UAV intended to work as S-BS, it will reduce the blockage percentage to a minimum as well as the interference and end-to-end latency. We also optimize the UAV S-BS to use the FSO as media propagation between every two hops whenever it is possible along the selected route, which in turn increase the backhauling capacity, reduce the overall route interference, and increase the SNR. In this paper, we proposed a hybrid solution to use one of these technology (FSO or RF), and we assumed that FSO channel fading is

Gamma–Gamma in the presence of the pointing error. The initial evaluation shows that the INUSH algorithm shows a significant enhancement of the traditional deep learning approaches.

ACKNOWLEDGEMENT

REFERENCES

[1] D. Yuan, H.-Y. Lin, J. Widmer, and M. Hollick, "Optimal joint routing and scheduling in millimeter-wave cellular networks," in *IEEE INFOCOM 2018 - IEEE Conference on Computer Communications*, 2018, pp. 1205–1213, doi: 10.1109/INFOCOM.2018.8485929.

[2] Q. Hu and D. M. Blough, "Relay selection and scheduling for millimeter wave backhaul in urban environments," in *2017 IEEE 14th International Conference on Mobile Ad Hoc and Sensor Systems (MASS)*, 2017, pp. 206–214, doi: 10.1109/MASS.2017.48.

[3] R. Taori and A. Sridharan, "Point-to-multipoint in-band mmwave backhaul for 5G networks," *IEEE Communications Magazine*, vol. 53, no. 1, pp. 195–201, Jan. 2015, doi: 10.1109/MCOM.2015.7010534.

[4] A. Ortiz, A. Asadi, G. H. Sim, D. Steinmetzer, and M. Hollick, "SCAROS: a scalable and robust self-backhauling solution for highly dynamic millimeter-wave networks," *IEEE Journal on Selected Areas in Communications*, vol. 37, no. 12, pp. 2685–2698, Dec. 2019, doi: 10.1109/JSAC.2019.2947925.

[5] M. Kamel, W. Hamouda, and A. Youssef, "Ultra-dense networks: a survey," *IEEE Communications Surveys and Tutorials*, vol. 18, no. 4, pp. 2522–2545, 2016, doi: 10.1109/COMST.2016.2571730.

[6] T. Ihalainen *et al.*, "Flexible scalable solutions for dense small cell networks," in *Proceedings Wireless World Research Forum (WWRF)*, 2013.

[7] A. Łukowa, V. Venkatasubramanian, and P. Marsch, "Dynamic self-backhauling in 5G networks," *2018 IEEE 29th Annual International Symposium on Personal, Indoor and Mobile Radio Communications (PIMRC)*, 2018, pp. 1–7, doi: 10.1109/PIMRC.2018.8580727.

[8] S. Niknam and B. Natarajan, "On the regimes in millimeter wave networks: noise-limited or interference-limited?," in *2018 IEEE International Conference on Communications Workshops (ICC Workshops)*, 2018, pp. 1–6, doi: 10.1109/ICCW.2018.8403515.

[9] D. Steinmetzer, D. Wegemer, M. Schulz, J. Widmer, and M. Hollick, "Compressive millimeter-wave sector selection in off-the-shelf IEEE 802.11ad devices," in *CoNEXT'17: Proceedings of the 13th International Conference on emerging Networking EXperiments and Technologies*, 2017, pp. 414–425, doi: 10.1145/3143361.3143384.

[10] A. Malik and P. Singh, "Free space optics: current applications and future challenges," *International Journal of Optics*, vol. 2015, 2015, doi: 10.1155/2015/945483.

[11] M. N. Kulkarni, A. Ghosh,, and J. Andrews, "How many hops can self-backhauled millimeterwave cellular networks support," *arXiv preprint arXiv:1805.01040*, 2018.

[12] Y. Zhu, Y. Niu, J. Li, D. O. Wu, Y. Li, and D. Jin, "QoS-aware scheduling for small cell millimeter wave mesh backhaul," in *2016 IEEE International Conference on Communications (ICC)*, 2016, pp. 1–6, doi: 10.1109/ICC.2016.7511065.

[13] J. Du, E. Onaran, D. Chizhik, S. Venkatesan, and R. A. Valenzuela, "Gbps user rates using mmwave relayed backhaul with high-gain antennas," *IEEE Journal on Selected Areas in Communications*, vol. 35, no. 6, pp. 1363–1372, Jun. 2017, doi: 10.1109/JSAC.2017.2686578.

[14] G. H. Sim, M. Mousavi, L. Wang, A. Klein, and M. Hollick, "Joint relaying and spatial sharing multicast scheduling for mmwave networks," in *2020 IEEE 21st International Symposium on "A World of Wireless, Mobile and Multimedia Networks" (WoWMoM)*, 2020, pp. 127–136, doi: 10.1109/WoWMoM49955.2020.00033.

[15] M. E. Rasekh, D. Guo, and U. Madhow, "Interference-aware routing and spectrum allocation for millimeter wave backhaul in urban picocells," in *2015 53rd Annual Allerton Conference on Communication, Control, and Computing (Allerton)*, 2015, pp. 1–7, doi: 10.1109/ALLERTON.2015.7557347.

[16] M. K. Haider and E. W. Knightly, "Mobility resilience and overhead constrained adaptation in directional 60 GHz WLANs: protocol design and system implementation," in *MobiHoc'16: Proceedings of the 17th ACM International Symposium on Mobile Ad Hoc Networking and Computing*, 2016, pp. 61–70, doi: 10.1145/2942358.2942380.

[17] S. Sur, X. Zhang, P. Ramanathan, and R. Chandra, "BeamSpy: enabling robust 60 GHz links under blockage," in *Proceedings of the 13th USENIX Symposium on Networked Systems Design and Implementation (NSDI '16)*, 2016.

[18] H. Hassanieh, O. Abari, M. Rodriguez, M. Abdelghany, D. Katabi, and P. Indyk, "Fast millimeter wave beam alignment," in *Proceedings of the 2018 Conference of the ACM Special Interest Group on Data Communication*, 2018, pp. 432–445, doi: 10.1145/3230543.3230581.

[19] A. Zhou, X. Zhang, and H. Ma, "Beam-forecast: facilitating mobile 60 GHz networks via model-driven beam steer-ing," in *IEEE INFOCOM 2017 - IEEE Conference on Computer Communications*, 2017, pp. 1-9, doi: 10.1109/IN-FOCOM.2017.8057188.

[20] A. Zhou, L. Wu, S. Xu, H. Ma, T. Wei, and X. Zhang, "Following the shadow: agile 3-D Beam-steering for 60 GHz wireless networks," in *IEEE INFOCOM 2018 - IEEE Conference on Computer Communications*, 2018, pp. 2375–2383, doi: 10.1109/INFOCOM.2018.8486399.

[21] "Study on integrated access and backhaul," Technical Specification Group Radio Access Network, 2018, Accessed: Apr. 22 Date. [Online]. Available: https://portal.3gpp.org/desktopmodules/Specifications/SpecificationDetails.aspx?specificationId=3232

[22] R. S. Sutton and A. G. Barto, *Reinforcement learning: an introduction*, 2nd Ed., MIT Press, 2017.

[23] A. Tahami, A. Dargahi, K. Abedi, and A. Chaman-Motlagh, "A new relay based architecture in hybrid RF/FSO system," *Physical Communication*, vol. 36, 2019, doi: 10.1016/j.phycom.2019.100818.

[24] W. Gappmair, "Further results on the capacity of free-space optical channels in turbulent atmosphere," *IET commu-nications*, vol. 5, no. 9, pp. 1262–1267, 2011, doi: 10.1049/iet-com.2010.0172.

[25] W. O. Popoola and Z. Ghassemlooy, "BPSK subcarrier intensity modulated free-space optical communica-tions in atmospheric turbulence," *Journal of Lightwave Technology*, vol. 27, no. 8, pp. 967–973, 2009, doi: 10.1109/JLT.2008.2004950..

[26] A. Jurado-Navas, J. M. Garrido-Balsells, J. F. Paris, M. Castillo-Vázquez, and A. Puerta-Notario, "Impact of pointing errors on theperformance of generalized atmosphericoptical channels," *Optic Express*, vol. 20. no. 11, 2012, doi: 10.1364/OE.20.012550.

BIOGRAPHIES OF AUTHORS

Mohammad A. Massad received the B.Sc. degree in Computer Science from Yarmouk University, Jordan, in 2004 and the M.Sc. degree in Network Engineering and Security from Jordan University of Science and Technology, Jordan, in 2021. Currently pursuing a Ph.D. degree in Computer Science at Queen's University, Canada. have 16+ years of professional experience in international and recognized companies. His research interests are next-generation cellular networks, wireless networks, internet of things (IoT), UAV networks and autonomous vehicles systems, edge and fog computing, and network security. He can be contacted at: mamassad18@cit.just.edu.jo.

Baha' Adnan Alsaify received his B.S. degree in Computer Engineering from the Jordan University of Science and Technology (JUST), Irbid, Jordan in 2007. He received his M.S. in Computer Engineering from the University of Arkansas (UARK), Fayetteville, AR, USA in 2009. He received his Ph.D. in Computer Engineering from the University of Arkansas, Fayetteville, AR, USA in 2012. He then joined the Computer Engineering Department of the Yarmouk University (YU), in Irbid, Jordan. In 2015, he joined the Jordan University of Science and Technology and he is currently an Assistant Professor at the Department of Network Engineering and Security (NES). His research interests are radio frequency identification (RFID), computer security, machine learning, human activity recognition, and computer networks. He can be contacted at: baalsaify@just.edu.jo.

Abdallah Y. Alma'aitah (Member, IEEE) received the B.Sc. degree in Computer Engineering from Mutah University, Jordan, in 2005 and the M.Sc. degree in Electrical and Computer Engineering from the University of Western Ontario, Canada in 2008, and the Ph.D. degree in Electrical and Computer Engineering from Queen's University, Canada, in 2013. Currently, he is an associate professor at the Department of Network Engineering and Security at Jordan University of Science and Technology. His research interests are fifth generation networks and emerging future networks, power and security management in power constrained networks, and UAV and autonomous vehicles systems. He can be contacted at: ayalmaaitah@just.edu.jo.